Supplemental Materials and Methods

Circular dichroism spectroscopy- Far-UV CD experiments were performed at 25º C on an Aviv 60 DS CD spectrophotometer. The spectrum of PDI and its variants at a concentration of 0.3 mg/ml in 20 mM Tris, pH 8.5 and 250 mM NaCl was recorded in 0.1 cm quartz cuvettes over a range from 201 to 260 nm at 1 nm intervals with an average scan time of 1 s. Five scans of each sample were averaged and the background spectrum of the buffer was subtracted from the averaged value.

Construction of yeast expression plasmids- To express PDI and its variants in yeast, either the pRS314 vector with a TRP1 selectable marker or the pRS315 vector with a Leu2 selectable marker (1) were modified by inserting a PDI specific expression cassette between the EcoRI and BamHI sites (Figure S1B). The cassette consisted of a 600-bp upstream fragment of the *PDI1* gene (-534 to +66), including residues 1-22 as the signal sequence, a 154-bp downstream fragment (+1555 to +1711) including the HDEL ER retention signal and a stop codon. A cloning site consisting of NdeI-XhoI-PstI was engineered between the signal sequence and the HDEL sequence. This design ensured that PDI and its variants are expressed under the native promoter of the *PDI1* gene and were targeted to the ER. The wild-type and point mutants of yeast PDI were cloned between the NdeI and PstI sites. For epitope tagging, the tag was linked to PDI at either terminus and inserted between the NdeI and PstI sites through three-fragment ligation (2) with XhoI as the central ligation site (Figure S1C). Flexible linkers made up of one or two copies of the sequence Gly-Gly-Gly-Gly-Ser were engineered between PDI and the tag.

Analytical ultracentrifugation- All sedimentation experiments were conducted using a Beckman XL-I Optima analytical ultracentrifuge and a Ti-60a rotor. For sedimentation velocity (S.V.) studies, two-channel, charcoal-filled epon centerpieces with quartz windows were filled with 410 µl reference buffer and 400 µl sample equilibrated with the same buffer. Absorbance profiles were collected at 280 nm with a radial step size of 0.003 cm at 40,000 rpm until no sedimentation was visible. For sedimentation equilibrium (S.E.) studies, six-channel centerpieces were used with 125 µl reference buffer and 120 µl sample in the same buffer. Absorbance profiles were collected at 280 nm with a radial step size of 0.001 cm at three different speeds. At each speed, the samples were scanned every 4 hours and were centrifuged for at least 20 hours. To ensure that equilibrium had been achieved the last two scans at each speed were overlapped using the XL-A/XL-I data analysis software (Beckman, Fullerton, CA). A series of sedimentation experiments was carried out under the conditions summarized in Table 3. The sedimentation velocity data were analyzed with SedFit (3) to obtain the distribution of sedimenting species. The oligomeric state of each species was judged based on its weighted average molecular weight. The standard sedimentation coefficients ($S_{20,w}$) were converted from the apparent sedimentation coefficients with Sednterp (4) and compared with the $S_{20,w}$ values predicted from the crystal structure by Hydropro (5). Sedimentation equilibrium data were analyzed with Heteroanalysis (National Analytical Ultracentrifugation Facility at the University of Connecticut) to find the best fitting model and the corresponding dissociation constants (K_D) at different concentrations were estimated by global fitting of all data from different speeds. All experiments were carried out in 20 mM Tris 8.5, 250 mM NaCl, with a calculated solvent density of 1.01088 g/cm^3 at 4° C and 1.00865 g/cm^3 at 22° C. The partial specific volume of PDI was approximated with Sednterp from the amino acid compositions as 0.7248 cm^3/g at 4° C and 0.7325 cm^3/g at 22° C.

Supplemental References

1. Sikorski, R. S., and Hieter, P. (1989) *Genetics* **122**, 19-27
2. Taghbalout, A., Ma, L., and Rothfield, L. (2006) *J Bacteriol* **188**, 2993-3001
3. Schuck, P. (2000) *Biophys J* **78**, 1606-1619
4. Laue, T. M., Shah, B. D., Ridgeway, T. M., and Pelletier, S. L. (1992) in *Analytical Ultracentrifugation in Biochemistry and Polymer Science* (Harding, S. E., Rowe, A. J., and Horton, J. C., ed), pp. 90-125, Royal Society of Chemistry, Cambridge
5. Garcia De La Torre, J., Huertas, M. L., and Carrasco, B. (2000) *Biophys J* **78**, 719-730

Supplemental Figures

Figure S1

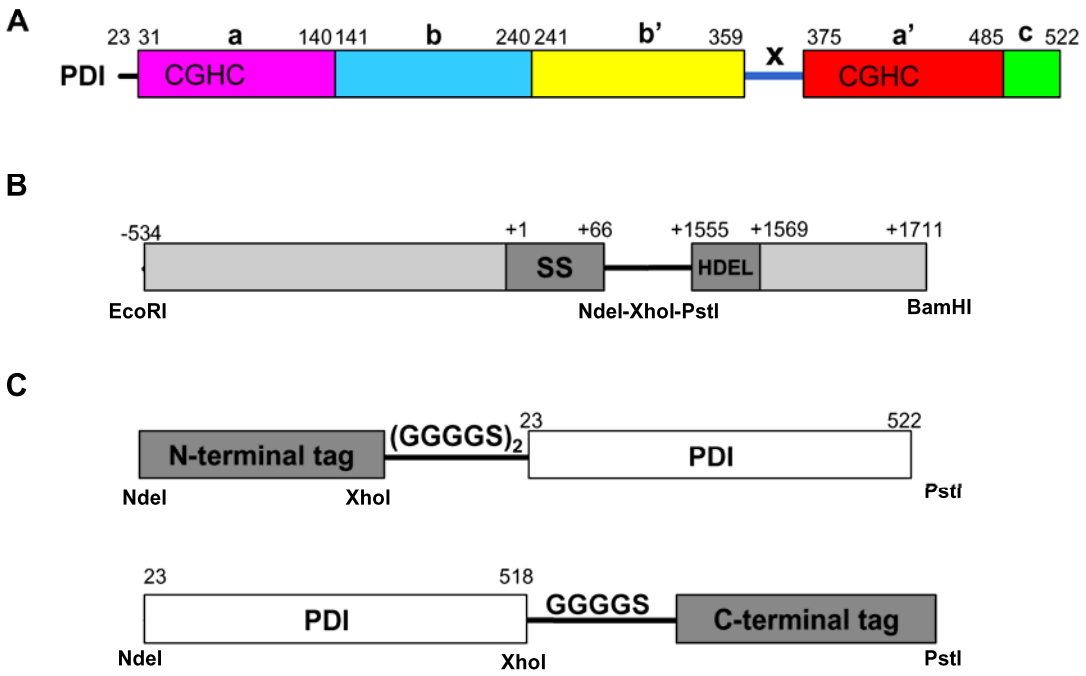

Fig. S1. **Primary structure of yeast PDI and schematic representation of PDI constructs**
(A) Primary structure of full-length yeast PDI (residues 23-522). Domain boundaries, which are defined based on the crystal structure and sequence alignments with thioredoxin, are marked. The Cys-Gly-His-Cys motifs indicate the location of the active sites and X the loop connecting the b' and a' domains.
(B) Nucleotide sequence of the PDI yeast expression cassette including an upstream sequence (-534 to -1), signal sequence (SS) (+1 to +66), NdeI-XhoI-PstI restriction sites, HDEL retention sequence and stop codon (+1555 to + 1569) as well as the downstream sequence (+1570 to +1711). This cassette was inserted between the EcoRI and BamHI sites of the pRS314 and pRS315 vectors.
(C) Tagged variants of PDI. Restriction sites utilized during the ligation as well as the residues of PDI used for tag attachment are marked. The sequence of flexible linkers located between each tag and PDI are indicated.

Figure S2

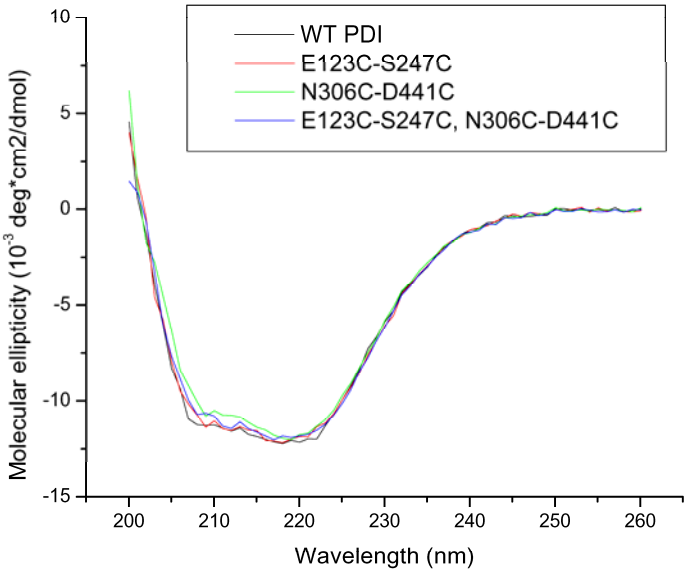

Figure S2. **Circular dichroism spectra of the "disulfide scan" mutants**
Far-UV circular dichroism (201 – 260 nm) spectra of wild type PDI and "disulfide-scan" mutants based on the "twisted U" conformation of PDI. The molecular ellipticity [θ] was calculated as follows: signal (mdeg) x 1000 / (cell length (cm) x concentration (M) x peptide bonds x 10) in units of $deg \cdot cm^2 \cdot dmol^{-1}$.

Figure S3

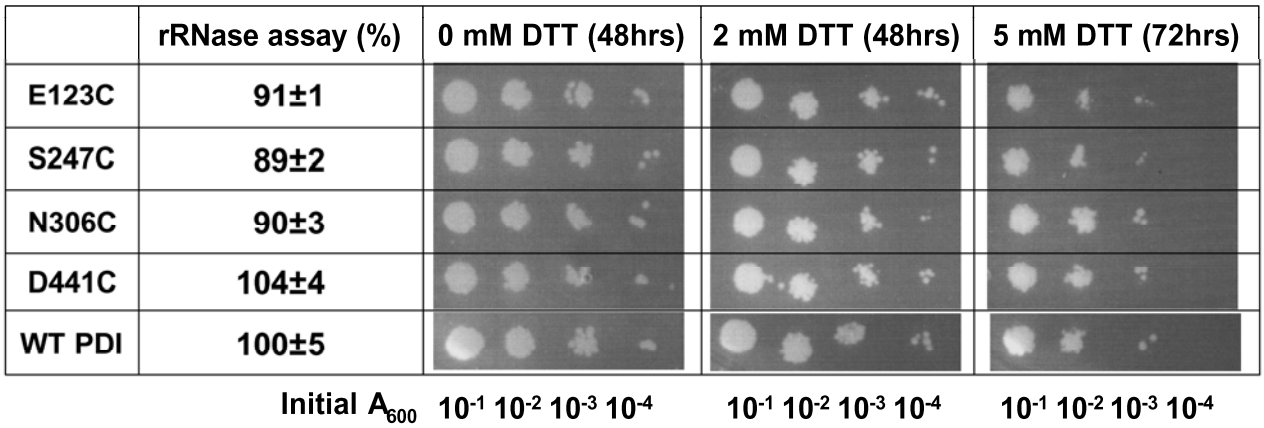

Figure S3. **Activity assays of PDI mutants containing the single cysteine substitutions within the "disulfide-scan" mutations**

The *in vitro* RNase refolding activity of the single-cysteine mutants was measured with reduced RNase (rRNase) as substrate and compared to wild-type PDI. The indicated standard deviations result from three independent experiments. The *in vivo* ability of these mutants to support cell growth under normal or stressed condition was compared with wild-type PDI in a spotting assay. The cells were grown in the absence and presence of DTT for the indicated time periods using four different initial cell concentrations.

Figure S4

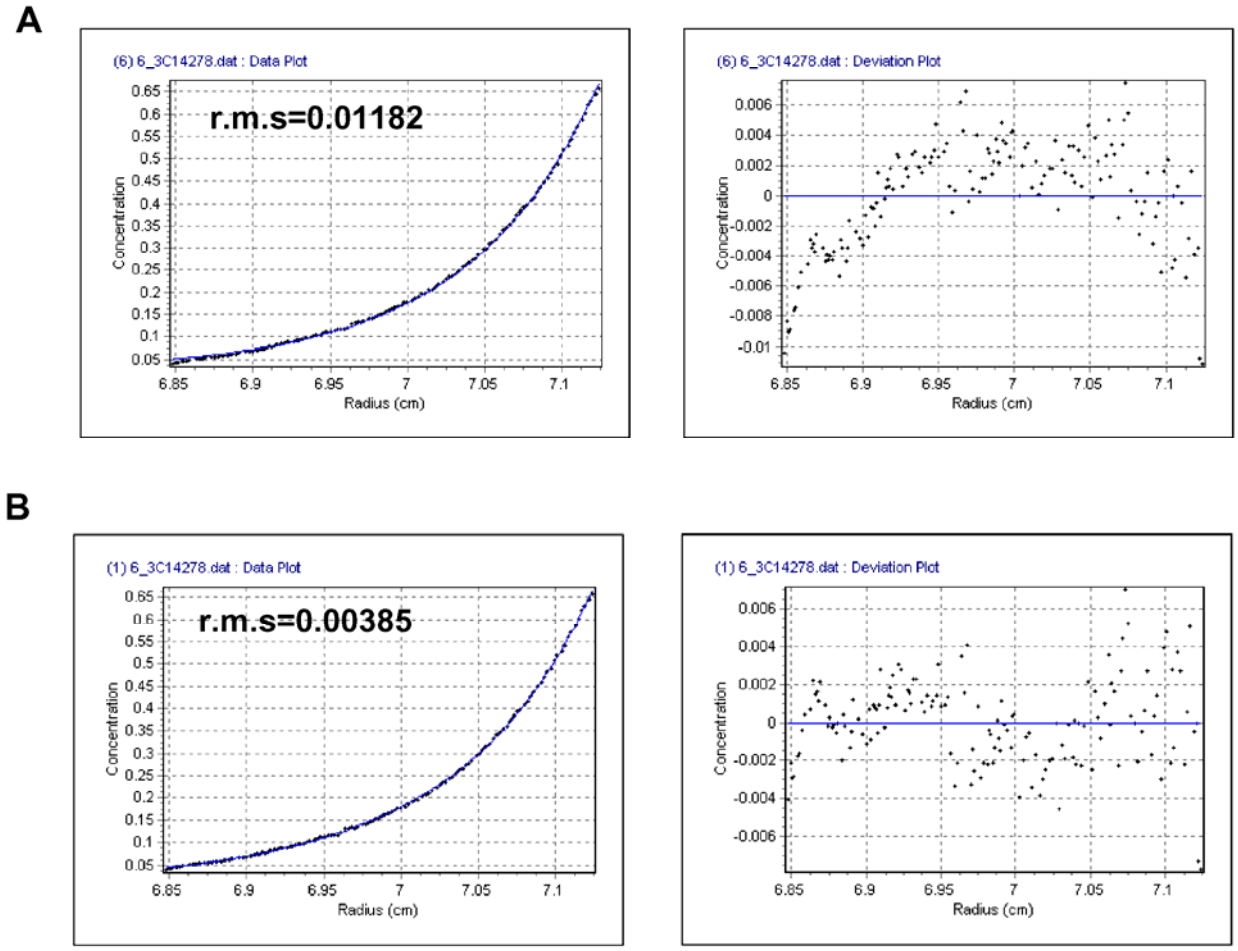

Figure S4. **Sedimentation equilibrium data of PDI**
Sedimentation equilibrium data for full-length PDI (0.2 mg/ml) obtained at 14,000 rpm after 32 h at 22° C, and fit to either a monomer model (A) or a monomer-dimer model (B). Left panel: crosses represent the experimental data, and the solid blue line the data calculated for each model. Right panel: Distribution of residuals between the experimental data (black crosses) against the model (blue line). Fitting with the monomer-dimer model results in smaller and more random deviations.